

## Supporting Information I

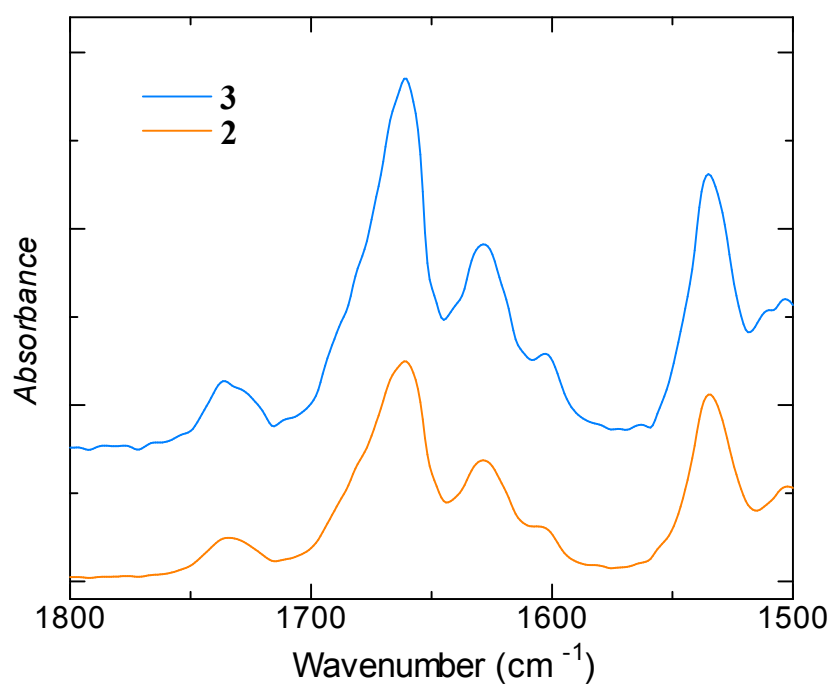
### Transfer of Noncovalent Chiral Information along an Optically Inactive Helical Peptide Chain: Allosteric Control of Asymmetry of the C-Terminal Site by External Molecule that Binds to the N-Terminal Site

Naoki Ousaka<sup>§</sup> and Yoshihito Inai<sup>†,\*</sup>

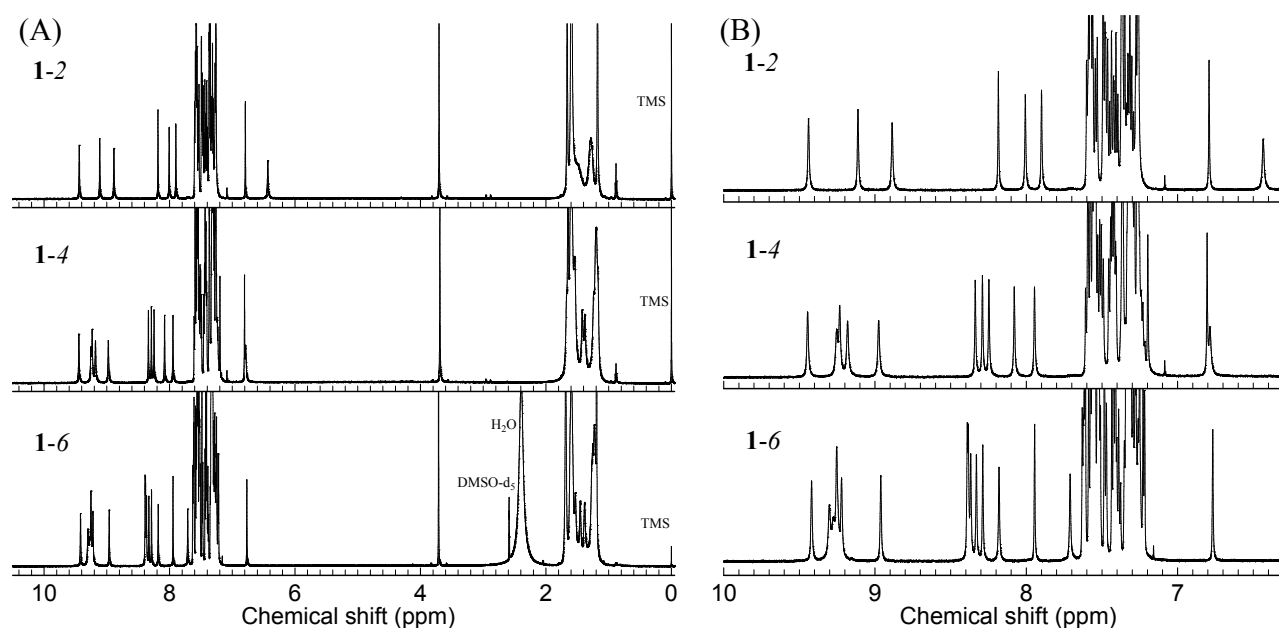
<sup>§</sup>Department of Environmental Technology and Urban Planning, <sup>†</sup>Department of Frontier Materials, Shikumi College, Graduate School of Engineering, Nagoya Institute of Technology, Gokiso-cho, Showa-ku, Nagoya 466-8555, Japan

\*Correspondence to Y. Inai (inai.yoshihito@nitech.ac.jp)

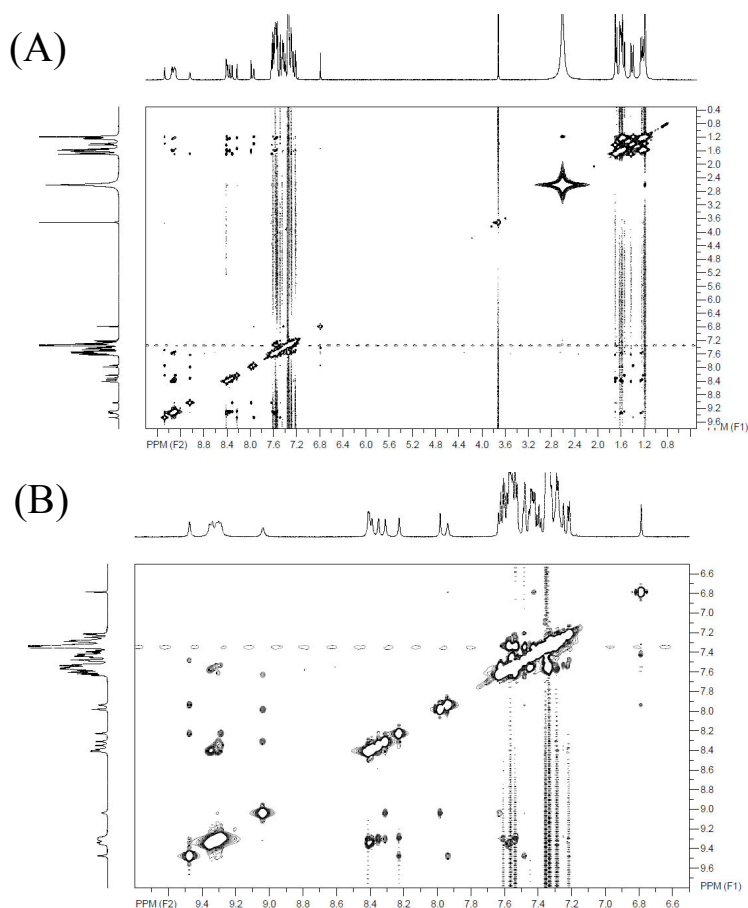
Contents	Pages
<b>Figure S1.</b> FT-IR absorption spectra of peptides <b>2</b> and <b>3</b> in chloroform.	S2
<b>Figure S2.</b> <sup>1</sup> H-NMR spectra of peptides <b>1-m</b> at 293 K.	S3
<b>Figure S3.</b> 2D NOESY spectra of peptide <b>1-6</b> in CDCl <sub>3</sub> /(CD <sub>3</sub> ) <sub>2</sub> SO (100/3.7, v/v%) at 273 K.	S3
<b>Figure S4.</b> 2D NOESY spectra of peptide <b>1-4</b> in CDCl <sub>3</sub> at 293 K.	S4
<b>Figure S5.</b> 2D NOESY spectra of peptide <b>1-2</b> in CDCl <sub>3</sub> at 293 K.	S4
<b>Figure S6.</b> Solvent-composition dependence of NH chemical shifts of <b>1-2</b> in CDCl <sub>3</sub> /(CD <sub>3</sub> ) <sub>2</sub> SO at 293 K.	S5
<b>Table S1.</b> Average values of selected torsion angles and hydrogen-bonding parameters of <b>1-m</b> in <sub>310</sub> -helix.	S5
<b>Figure S7.</b> Right-handed helical structures of <b>1-m</b> energy-minimized from an $\alpha$ -helix: (A, B) <b>1-6</b> , (C, D) <b>1-4</b> , and (E, F) <b>1-2</b> .	S6
<b>Figure S8.</b> CD spectra of peptides <b>2</b> or <b>3</b> with and without Boc-L-Pro-OH in chloroform.	S7
<b>Figure S9.</b> Induced CD spectra of peptides <b>1-m</b> with Boc-D-Pro-OH or Boc-L-Pro-OH.	S7
<b>Figure S10.</b> CD spectra of Boc-protected <b>1-m</b> [Boc-(Aib- $\Delta^Z$ Phe) <sub>m</sub> -(Aib- $\Delta^Z$ Bip) <sub>2</sub> -Aib-OMe] and with Boc-L-Pro-OH in chloroform.	S7
<b>Figure S11.</b> Relationship between the induced CD intensity ( $\Delta\epsilon$ of <b>1-m</b> and <b>2</b> ) and Boc-L-Pro-OH concentration in chloroform at ambient temperature.	S8
<b>Figure S12.</b> Spatial arrangements of each $\Delta$ AA residue TDM (in the length form) along the right-handed <sub>310</sub> -helix.	S8



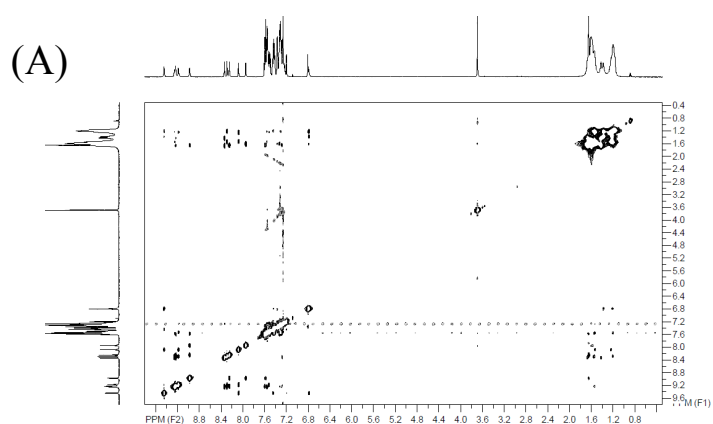
**Figure S1.** FT-IR absorption spectra of peptides **2** and **3** in chloroform at ambient temperature: [**2**] = 1 mM; [**3**] = 1.8 mM.



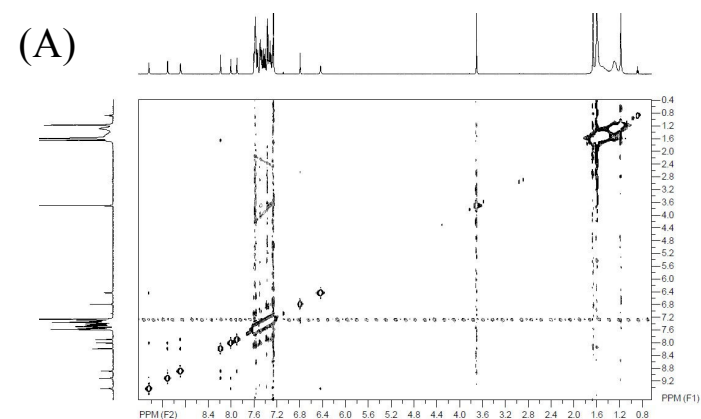
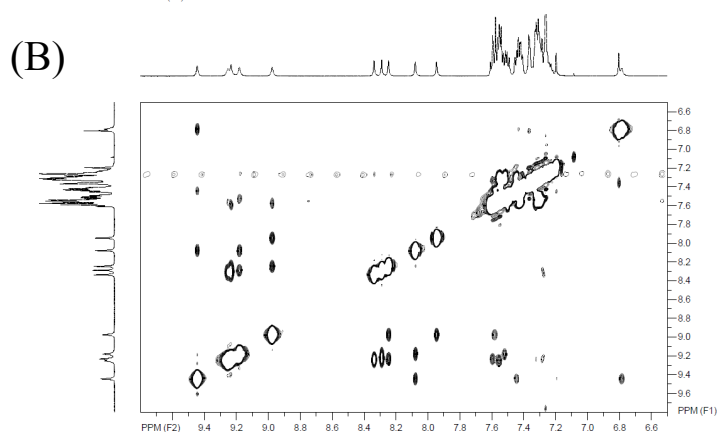
**Figure S2.**  $^1\text{H}$ -NMR spectra of peptides **1-m** in (A) a wide range and (B) an expanded scale: at 293 K; [peptide] = 3 mM;  $\text{CDCl}_3$  for  $m = 2$  and 4;  $\text{CDCl}_3/(\text{CD}_3)_2\text{SO}$  (100/3.7, v/v%) for  $m = 6$ .



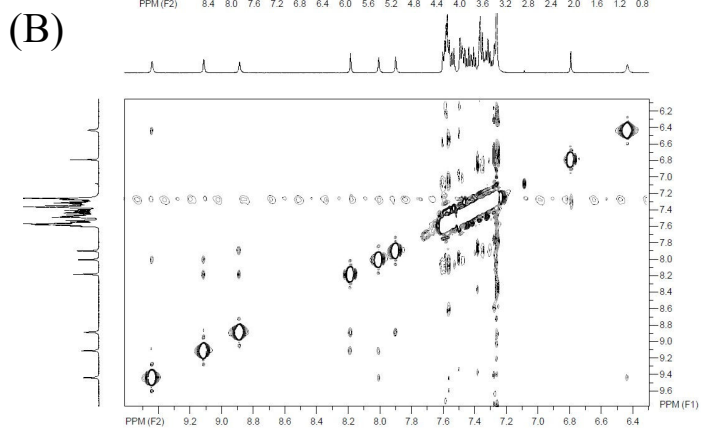
**Figure S3.** 2D NOESY spectra of peptide **1-6** in  $\text{CDCl}_3/(\text{CD}_3)_2\text{SO}$  (100/3.7, v/v%) at 273 K: (A) wide region; (B) NH and aromatic region. [**1-6**] = 3 mM (prepared at room temperature); mixing time = 0.2 s.



**Figure S4.** 2D NOESY spectra of peptide 1-4 in  $\text{CDCl}_3$  at 293 K: (A) wide region; (B) NH and aromatic region.  $[\mathbf{1-4}] = 3 \text{ mM}$ ; mixing time = 0.4 s.



**Figure S5.** 2D NOESY spectra of peptide 1-2 in  $\text{CDCl}_3$  at 293 K: (A) wide region; (B) NH and aromatic region.  $[\mathbf{1-2}] = 3 \text{ mM}$ ; mixing time = 0.4 s.



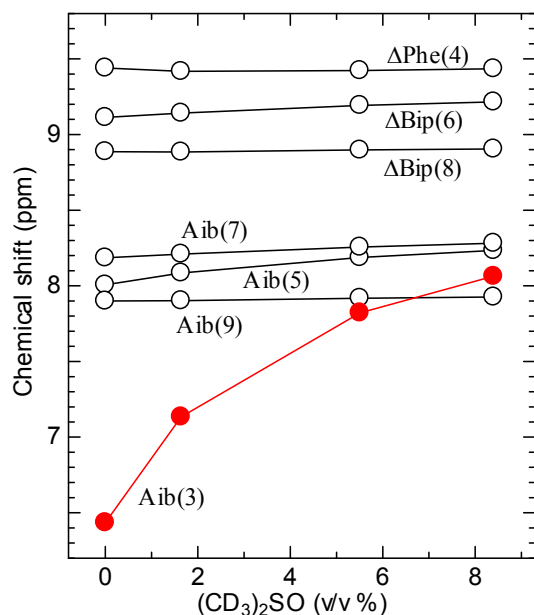


**Figure S6.** Solvent-composition dependence of NH chemical shifts of **1-2** in  $\text{CDCl}_3/(\text{CD}_3)_2\text{SO}$  at 293 K:  $[\mathbf{1-2}] = 3 \text{ mM}$  [prior to the addition of  $(\text{CD}_3)_2\text{SO}$ ].

**Table S1.** Average values of selected torsion angles and hydrogen-bonding parameters of **1-*m*** in  $3_{10}$ -helix

peptide <sup>a</sup>	helix type	Bip <sup>b</sup>	torsion angles							hydrogen-bonding parameters				
			residues for average	$\phi$	$\psi$	$\omega$	$\chi^1$	$\chi^2$	$\chi^6$	hydrogen-bonding type/range	$\text{O}\cdots\text{H}$ (Å)	$\text{O}\cdots\text{N}$ (Å)	$\text{C}=\text{O}\cdots\text{H}$ (°)	$\text{O}\cdots\text{H}-\text{N}$ (°)
<b>1-6</b>	$3_{10}$ -helix	P	2–16	-41	-40	178	-2.5	-45	40	$(i)_{\text{CO}}\leftarrow(i+3)_{\text{NH}}$ : from $[1 \leftarrow 4]$ to $[14 \leftarrow 17]$	2.2	3.1	141	161
	$3_{10}$ -helix	M	2–16	-41	-40	178	-2.6	-45	-40	$(i)_{\text{CO}}\leftarrow(i+3)_{\text{NH}}$ : from $[1 \leftarrow 4]$ to $[14 \leftarrow 17]$	2.2	3.1	141	161
<b>1-4</b>	$3_{10}$ -helix	P	2–12	-41	-40	178	-2.6	-45	40	$(i)_{\text{CO}}\leftarrow(i+3)_{\text{NH}}$ : from $[1 \leftarrow 4]$ to $[10 \leftarrow 13]$	2.2	3.1	141	161
	$3_{10}$ -helix	M	2–12	-41	-40	178	-2.6	-45	-40	$(i)_{\text{CO}}\leftarrow(i+3)_{\text{NH}}$ : from $[1 \leftarrow 4]$ to $[10 \leftarrow 13]$	2.2	3.0	142	161
<b>1-2</b>	$3_{10}$ -helix	P	2–12	-40	-40	177	-2.6	-46	40	$(i)_{\text{CO}}\leftarrow(i+3)_{\text{NH}}$ : from $[1 \leftarrow 4]$ to $[6 \leftarrow 9]$	2.2	3.1	142	160
	$3_{10}$ -helix	M	2–12	-40	-40	177	-2.5	-45	-39	$(i)_{\text{CO}}\leftarrow(i+3)_{\text{NH}}$ : from $[1 \leftarrow 4]$ to $[6 \leftarrow 9]$	2.2	3.1	143	160

<sup>a</sup>These conformations correspond to Figure 3 and Table 2 ( $3_{10}$ -helices). <sup>b</sup>biphenyl orientation ( $\chi^6$ ).

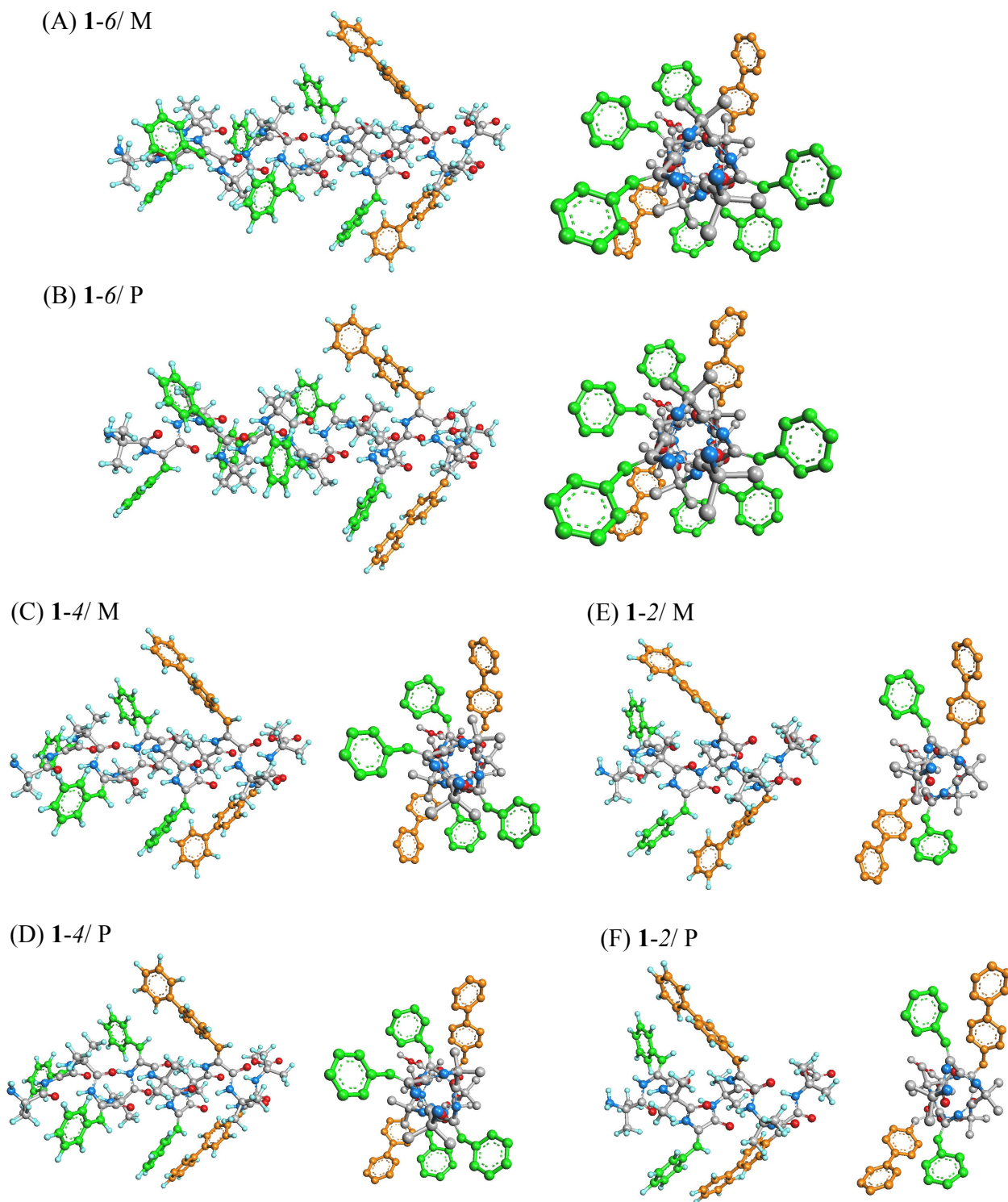


**Figure S7.** Right-handed helical structures of **1-*m*** energy-minimized from an  $\alpha$ -helix: (A, B) **1-6**, (C, D) **1-4**, and (E, F) **1-2**. M and P stand for the two orientations ( $\chi^6$ ) of the biphenyl groups.

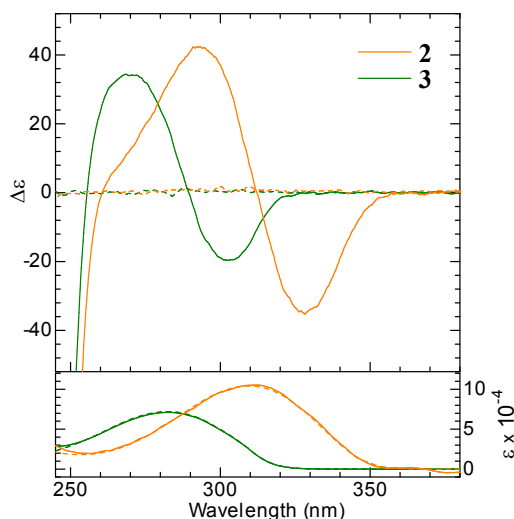


**Figure S8.** CD spectra of peptides **2** or **3** with (solid line) and without (broken line) Boc-L-proline in chloroform: [**2**] = 0.1 mM; [**3**] = 0.15 mM. CD and absorption spectra of **3** were also reported in ref 10a.

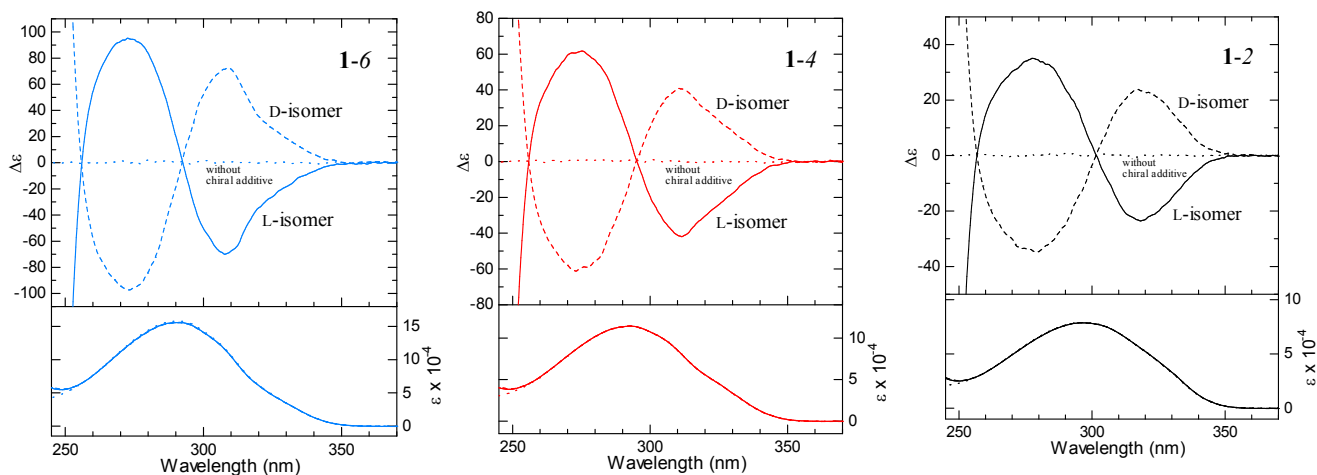


**Figure S9.** Induced CD spectra of peptides **1-m** with Boc-D-proline or Boc-L-proline. The spectra for Boc-L-proline and for no chiral additive correspond to Figure 4.

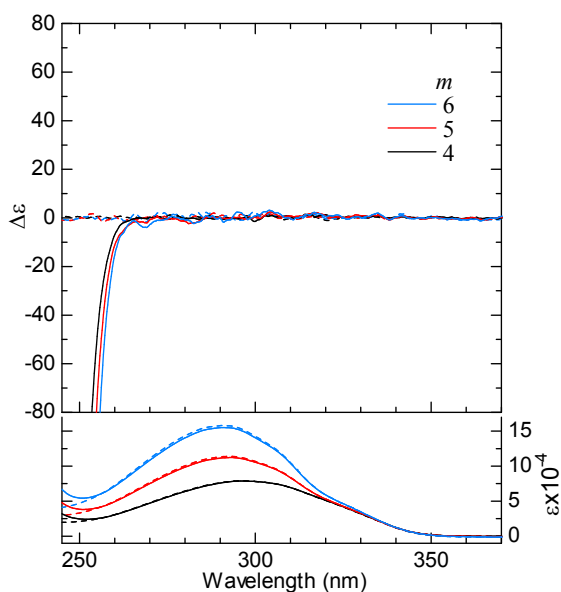


**Figure S10.** CD spectra of Boc-protected **1-m** [Boc-(Aib- $\Delta^Z$ Phe)<sub>m</sub>-(Aib- $\Delta^Z$ Bip)<sub>2</sub>-Aib-OMe] (broken line) and with Boc-L-proline (solid line) in chloroform: [**1-2**] = 0.13 mM; [**1-4**] =  $8.9 \times 10^{-2}$  mM; [**1-6**] =  $6.2 \times 10^{-2}$  mM; [Boc-L-proline] =  $1.5 \times 10^{-2}$  mM.

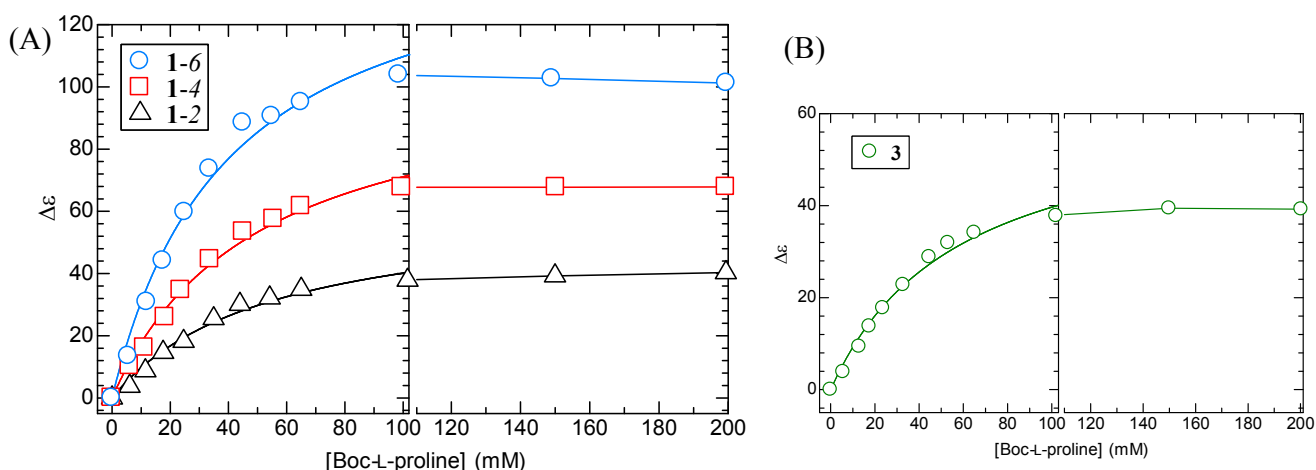


**Figure S11.** (A) Relationship between the induced CD intensity ( $\Delta\epsilon$ ) and Boc-L-proline concentration in chloroform at ambient temperature:  $[1-6] = 6.3 \times 10^{-2}$  mM;  $[1-4] = 9.0 \times 10^{-2}$  mM;  $[1-2] = 1.3 \times 10^{-1}$  mM. The CD intensity indicated  $\Delta\epsilon$  value at 272.8 nm (1-6), 274.8 nm (1-4), and 278.4 nm (1-2). In the left panel, the curve was obtained from nonlinear fitting for estimation of the binding constant (see ref 39). (B) A similar experiment for 3–Boc-L-proline monitoring  $\Delta\epsilon$  at 270 nm:  $[3] = 0.15$  mM. (The concentration dependence of chiral additive was similar to that already reported in ref 10a.) In (A) and (B),  $\Delta\epsilon$  value at [Boc-L-proline] = 0 mM was treated as zero.

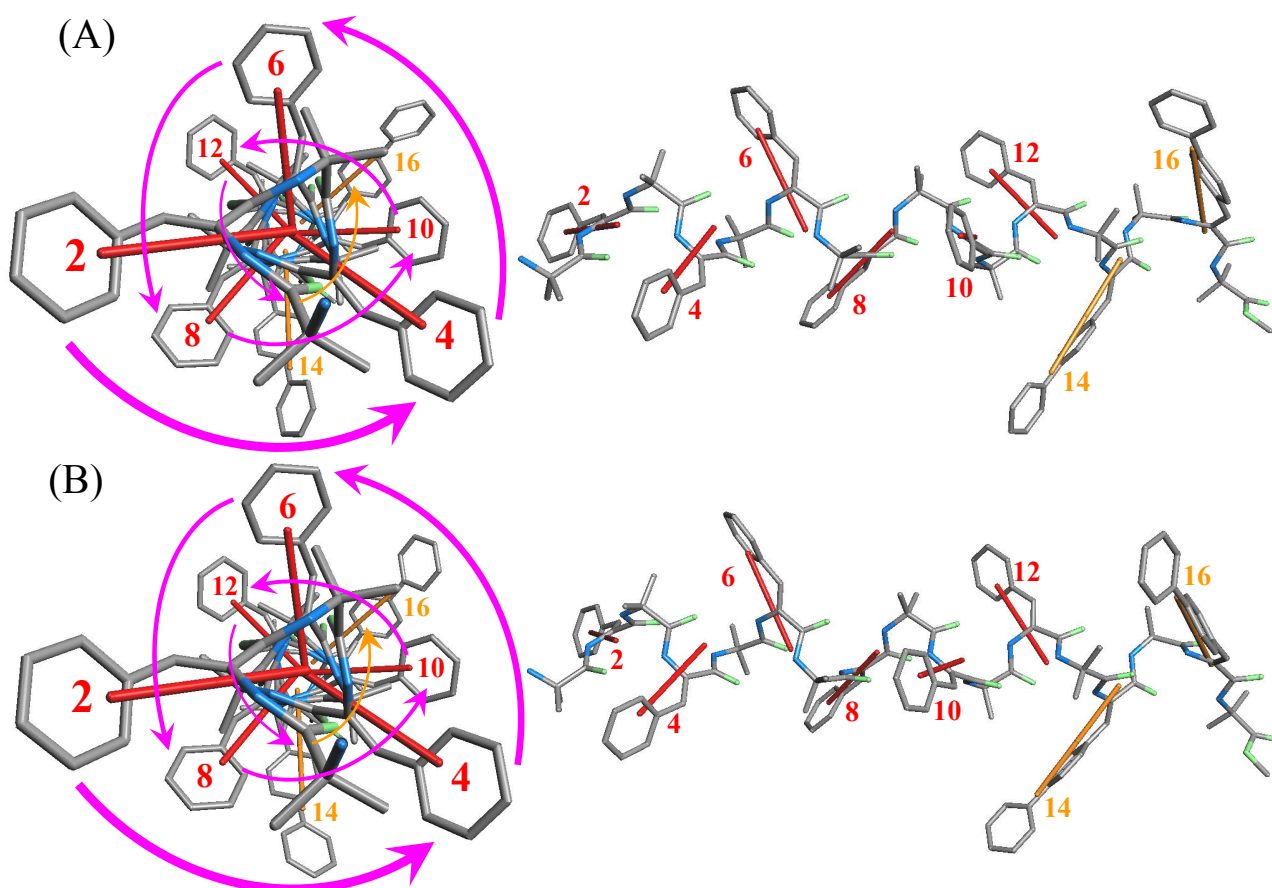


**Figure S12.** Spatial arrangement of each  $\Delta$ AA residue TDM (in the length form) along the right-handed  $3_{10}$ -helix of 1-6: (A) and (B) correspond to Figures 3A and 3B with the two types of  $\Delta^2$ Bip side-chain orientations. The right-handed helix produces a left-handed twist of the neighboring moments with respect to the helical axis.